REPORT DOCUMENTATION PAGE

Form Approved OMB NO. 0704-0188

1. REPORT DATE (DD-MM-YYYY)	2. REPORT TYPE	3. DATES COVERED (From - To)
06-07-2015	Final Report	1-Sep-2013 - 31-Aug-2016

4. TITLE AND SUBTITLE

Final Report: Numerical Simulation of Atmospheric Boundary Layer Flow Over Battlefield-scale Complex Terrain: Surface Fluxes From Resolved and Subgrid Scales

5a. CONTRACT NUMBER
W911NF-13-1-0474

5b. GRANT NUMBER

5c. PROGRAM ELEMENT NUMBER
611102

6. AUTHORS
William Anderson

5d. PROJECT NUMBER

5e. TASK NUMBER

5f. WORK UNIT NUMBER

7. PERFORMING ORGANIZATION NAMES AND ADDRESSES
Baylor University
One Bear Place 97360

Waco, TX 76798 -7360

8. PERFORMING ORGANIZATION REPORT NUMBER

9. SPONSORING/MONITORING AGENCY NAME(S) AND ADDRESS (ES)

U.S. Army Research Office
P.O. Box 12211
Research Triangle Park, NC 27709-2211

10. SPONSOR/MONITOR'S ACRONYM(S)
ARO

11. SPONSOR/MONITOR'S REPORT NUMBER(S)
63209-EV.1

12. DISTRIBUTION AVAILIBILITY STATEMENT

Approved for Public Release; Distribution Unlimited

13. SUPPLEMENTARY NOTES

The views, opinions and/or findings contained in this report are those of the author(s) and should not contrued as an official Department of the Army position, policy or decision, unless so designated by other documentation.

14. ABSTRACT

The large-eddy simulation (LES) tool has been used to study the transient characteristics of turbulent mixing in atmospheric boundary layer (ABL) flows over canonical topographies representative of complex, urban environments. Specifically, distributions of uniform height, staggered cubes are considered with heights equal to one quarter and one eighth of the ABL depth. An immersed boundary method has been implemented within the LES, to represent the presence of the cubes; this enables the computational domain to capture the classical roughness sublayer and aloft inertial layer. With this, time series of fluctuating streamwise and vertical velocity is

15. SUBJECT TERMS

16. SECURITY CLASSIFICATION OF:			17. LIMITATION OF ABSTRACT	15. NUMBER OF PAGES	19a. NAME OF RESPONSIBLE PERSON
a. REPORT	b. ABSTRACT	c. THIS PAGE			William Anderson
UU	UU	UU	UU		19b. TELEPHONE NUMBER 972-883-4660

Report Title

Final Report: Numerical Simulation of Atmospheric Boundary Layer Flow Over Battlefield-scale Complex Terrain: Surface Fluxes From Resolved and Subgrid Scales

ABSTRACT

The large-eddy simulation (LES) tool has been used to study the transient characteristics of turbulent mixing in atmospheric boundary layer (ABL) flows over canonical topographies representative of complex, urban environments. Specifically, distributions of uniform height, staggered cubes are considered with heights equal to one quarter and one eighth of the ABL depth. An immersed boundary method has been implemented within the LES, to represent the presence of the cubes; this enables the computational domain to capture the classical roughness sublayer and aloft inertial layer. With this, time series of fluctuating streamwise and vertical velocity is recorded over the ABL depth at various positions. Thus, the code has been used to record datasets that would more typically be recorded with micrometeorological instrumentation in field campaigns. However the unique spatial and temporal accessibility offered via simulations facilitates novel analysis that has led to new physical insights regarding the transient characteristics of roughness sublayer dynamics. It has been shown periods of momentum excess(deficit) in the inertial layer precede excitation(subdual) of cube-scale coherent vortices in the roughness sublayer, and a physics-based predictive model for the observed advective lag has been developed.

Enter List of papers submitted or published that acknowledge ARO support from the start of the project to the date of this printing. List the papers, including journal references, in the following categories:

(a) Papers published in peer-reviewed journals (N/A for none)

Received		Paper
07/06/2015	2.00	William Anderson. Passive scalar roughness lengths for atmospheric boundary layer flow over complex, fractal topographies, Environmental Fluid Mechanics, (02 2013): 1. doi:
07/06/2015	3.00	William Anderson, Qi Li, Elie Bou-Zeid. Numerical simulation of flow overurban-like topographies and evaluationof turbulence temporal attributes, Journal of Turbulence, (05 2015): 809. doi:
TOTAL:	**2**	

Number of Papers published in peer-reviewed journals:

(b) Papers published in non-peer-reviewed journals (N/A for none)

Received		Paper
TOTAL:		

Number of Papers published in non peer-reviewed journals:

(c) Presentations

Invited Seminars in which ARO-supported research was presented:

January 2014: University of Texas at Dallas, Mechanical Engineering Department, Dallas, TX.

January 2014: Los Alamos National Laboratory, Center for Nonlinear Studies, Los Alamos, NM.

February 2014: Sandia National Laboratory, Albuquerque, NM.

February 2014: University of Texas at Austin, Department of Aerospace Engineering and Engineering Mechanics, Austin, TX.

March 2014: University of Illinois at Urbana-Champaign, Department of Mechanical Science and Engineering, Champaign, IL.

March 2014: Shell Techology Center Houston, Houston, TX.

May 2014: Texas Tech University, Summer Research Unstitute, Lubbock, TX.

August 2014: Army Research Laboratory, Adelphi, MD.

Conference Presentations in which ARO-supported research was presented:

Li, Anderson, Bou-Zeid, Grimmond, 2015: Proc. 9th International Conference on Urban Climate, Paris, France.

Anderson W, Li Q, Bou-Zeid E, 2014: Proc. of American Geophysical Union, Fall Meeting, San Francisco, CA

Li Q, Bou-Zeid E, Anderson W, Grimmond S, 2014: Proc. of American Physical Society, Division of Fluid Dynamics, San Francisco, CA

Anderson W, Li Q, Bou-Zeid E, 2014: Proc. of American Physical Society, Division of Fluid Dynamics, San Francisco, CA

Anderson W, Li Q, Bou-Zeid E, 2014: Proc. of American Meteorological Society, Symposium on Boundary Layers and Turbulence, Leeds, CA

Li Q, Bou-Zeid E, Anderson W, 2014: Proc. of American Meteorological Society, Atlanta, GA

Number of Presentations: 0.00

Non Peer-Reviewed Conference Proceeding publications (other than abstracts):

Received	Paper

TOTAL:

Number of Non Peer-Reviewed Conference Proceeding publications (other than abstracts):

Peer-Reviewed Conference Proceeding publications (other than abstracts):

Received Paper

TOTAL:

Number of Peer-Reviewed Conference Proceeding publications (other than abstracts):

(d) Manuscripts

Received Paper

TOTAL:

Number of Manuscripts:

Books

Received Book

TOTAL:

Received	Book Chapter

TOTAL:

Patents Submitted

Patents Awarded

Awards

Graduate Students

NAME	PERCENT_SUPPORTED

FTE Equivalent:
Total Number:

Names of Post Doctorates

NAME	PERCENT_SUPPORTED

FTE Equivalent:
Total Number:

Names of Faculty Supported

NAME	PERCENT_SUPPORTED

FTE Equivalent:
Total Number:

Names of Under Graduate students supported

NAME	PERCENT_SUPPORTED

FTE Equivalent:
Total Number:

Student Metrics

This section only applies to graduating undergraduates supported by this agreement in this reporting period

The number of undergraduates funded by this agreement who graduated during this period: 0.00

The number of undergraduates funded by this agreement who graduated during this period with a degree in science, mathematics, engineering, or technology fields:..... 0.00

The number of undergraduates funded by your agreement who graduated during this period and will continue to pursue a graduate or Ph.D. degree in science, mathematics, engineering, or technology fields:..... 0.00

Number of graduating undergraduates who achieved a 3.5 GPA to 4.0 (4.0 max scale):..... 0.00

Number of graduating undergraduates funded by a DoD funded Center of Excellence grant for Education, Research and Engineering:..... 0.00

The number of undergraduates funded by your agreement who graduated during this period and intend to work for the Department of Defense 0.00

The number of undergraduates funded by your agreement who graduated during this period and will receive scholarships or fellowships for further studies in science, mathematics, engineering or technology fields: 0.00

Names of Personnel receiving masters degrees

NAME

Total Number:

Names of personnel receiving PHDs

NAME

Total Number:

Names of other research staff

NAME PERCENT_SUPPORTED

FTE Equivalent:

Total Number:

Sub Contractors (DD882)

Inventions (DD882)

Scientific Progress

See Attachment

Technology Transfer

FINAL REPORT: Grant # W911NF-13-1-0474

Numerical simulation of atmospheric boundary layer flow over battlefield-scale complex terrain: surface fluxes from resolved and subgrid scales

A final report submitted to the Army Research Office, Environmental Sciences Directorate, Atmospheric Sciences Program (Grant # W911NF-13-1-0474; PM: Dr. S. Collier, Dr. G. Videen)

PI: William Anderson, Mechanical Engineering Department, University of Texas at Dallas

1 Background

This document presents a summary of activities during Year # 1 of Grant # W911NF-13-1-0474 (FY2014). The funding period began in September, 2013, when the PI was at Baylor University. As discussed more extensively in Section 6, the PI moved from Baylor to the University of Texas at Dallas (UTD) in July, 2014. This professional move has affected the project by forcing the "Basic Award" to in fact conclude at Baylor, while a new start basic award will begin at UTD in October, 2014, for a duration of two years. This notwithstanding, the Year # 1 research effort has been remarkably successful. When the original proposal was submitted to then-PM Dr. Gorden Videen (Spring, 2012), PI Anderson had proposed to develop numerical treatments for fluxes of momentum and scalars in turbulent atmospheric surface layer flows over complex topographies at "battlefield scales" $\sim \mathcal{O}(10 \text{ km})$. This work was effectively following on from Anderson's PhD studies at Johns Hopkins University [1, 2]. The work was motivated by limitations of present computing resources for modeling microscale atmospheric flows (with large-eddy simulation, LES) and accounting for the full spectrum of topographic modes typical of a natural terrain. For example, Figure 1(a) shows a digital elevation map from Mason County, Texas, retrieved from the United States Geological Survey `seamless` server. The horizontal domains are $(L_x, L_y) \approx (10 \text{ km}, 10 \text{ km})$. The fine-grained height field (Figure 1a) is resolved at $\Delta_f = 3$ m. LES with resolution sufficiently fine to represent these small topographic scales while still capturing the largest ABL turbulent structures would require significant (perhaps prohibitively large) scientific computing resources. Consider then the effect of filtering the height field at a scale more appropriate in LES with this domain size, $\Delta_{LES} = 96$ m, Figure 1b. These images demonstrate that: (*i*) filtering removes important information from the height field; (*ii*) the landscape roughness is heterogeneous; and (*iii*) fluvial landscapes are characterized by branching, fractal-like channel networks [3]. We note that the choice of location for Figure 1 is arbitrary. While Anderson's preliminary efforts [1, 2] have focused on complex topographies most like that shown in Figure 1, one could also imagine addressing for example flows over partially resolved urban environments[4, 5, 6], or vegetative canopies[7, 8, 9, 10].

As a PhD student at Johns Hopkins, Anderson worked with PhD adviser (C. Meneveau) to develop models for momentum fluxes (that is, aerodynamic drag) associated with unresolved topographic modes in the Figure 1(b) topography. This was accomplished by first supposing that the total aerodynamic drag (i.e. due to $h(x, y)$) could be decomposed into that imposed by the filtered ($\tilde{h}(x, y)$) and unresolved ($h'(x, y)$) components:

$$F_i^{\Delta} \;=\; -\int_S \tilde{p}^w \; \tilde{n}_i \; dS + \rho \int_S \tau_{i3}^{w,\Delta} \; \tilde{n}_j \; dS, \tag{1}$$

where $\tilde{n}_i$ is the unit vector normal to the filtered landscape, $\tilde{h}(x,y)$, and $\tilde{p}^w$ is the resolved wall pressure acting on $\tilde{h}(x,y)$, while drag forces due to $h'(x,y)$ are represented by the equilibrium logarithmic law:

$$\frac{\tau_{13}^{w,\Delta}}{\rho} = u_\tau^2 \frac{\tilde{u}}{U} = -\left[\frac{\kappa U}{\log(z/z_0)}\right]^2 \frac{\tilde{u}}{U}, \tag{2}$$

where z_0 is a momentum roughness length, κ is the von Kármán constant, u_τ is the shear velocity, and U is magnitude of the horizontal components of the velocity vector*. Next, we invoke a self-consistency argument (the Germano identity[11]) on the plane-averaged aerodynamic drag at a grid- and test-filter scale; this is, we enforce that the total drag embodied in Equation 1 should be invariant to the filter resolution (assuming that the filter range is in the "inertial" range of the topography[1, 2]). Thus, one could imagine a test-filtered version of Equation 1:

$$F_i^{2\Delta} \;=\; -\int_S \widehat{\tilde{p}}^w \, \widehat{\tilde{n}}_i \, dS + \rho \int_S \tau_{i3}^{w,2\Delta} \, \widehat{\tilde{n}}_j \, dS, \tag{3}$$

where $\widehat{\ldots}$ denotes a test-filtered (more smooth) quantity. The self-consistency argument:

$$\langle F_i^{\Delta} \rangle = \langle F_i^{2\Delta} \rangle, \tag{4}$$

states that the averaged aerodynamic drag is equivalent, regardless of the choice of filter width, Δ. Thus, as Δ is varied, the drag imposed by the subgrid and resolved scales should change systematically such that the net quantity is preserved. Equation 4 is insightful, since it also allows one to inform parameters needed to parameterize the subgrid-scale roughness length, z_0. For brevity, additional details regarding the Equations 1 to 4 development are excluded here (Anderson has presented this work many times, including during an invited talk at the Army Research Laboratory Headquarters in Adelphi, MD in July, 2013).

It was originally anticipated that the 1 to 4 development would be applied analogously to model surface fluxes of passive scalars for Figure 1-like complex topographies. As a first stage effort, we sought to study the passive scalar surface flux characteristics of flow over a fully-resolved fractal-like topography. The equilibrium logarithmic law expression for passive scalar fluxes, $\dot{q}''$ (neutral stratification – stability correction terms not needed[12, 13]) is:

$$\frac{\dot{q}''}{\rho c_p} = \theta_\tau u_\tau = \frac{\kappa(\theta_s - \theta)}{\log(z/z_{0S})} u_\tau, \tag{5}$$

where θ_τ is shear temperature, z_{0S} is scalar roughness length, c_p is specific heat, θ_s is the surface temperature, and θ is passive quantity (for example, temperature in the absence of *large* thermal gradients). A large body of literature exists regarding values of z_{0S} [14, 15, 16, 17, 18, 19, 20, 21] in terms of the momentum roughness length,

$$z_{0S} = z_0 \exp\left[-\kappa\left(St_0^{-1} - Cd_0^{-1/2}\right)\right], \tag{6}$$

*In this report, we adopt the following nomenclature: $\boldsymbol{x} = \{x, y, z\}$ correspond with the streamwise, spanwise, and vertical positions, respectively; $\tilde{\boldsymbol{u}} = \{\tilde{u}, \tilde{v}, \tilde{w}\}$ correspond with the streamwise, spanwise, and vertical velocity components, respectively.

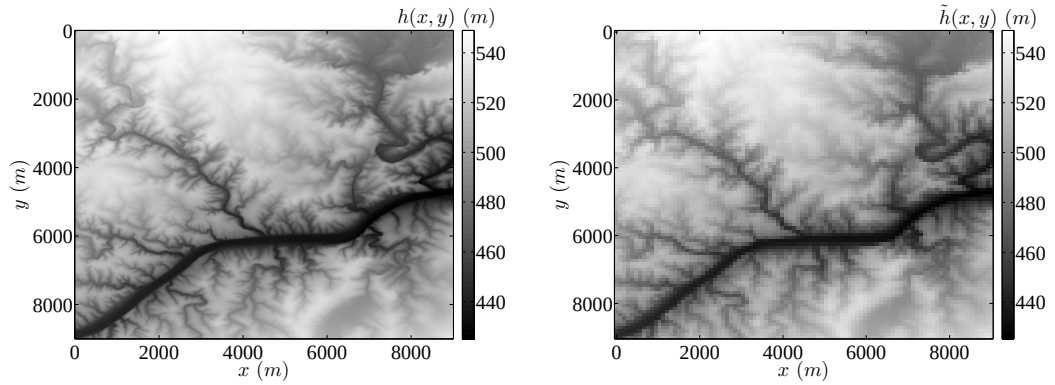

Figure 1: Contour view of height distribution at 30.57° : 30.77° N and -99.22° : -99.47° E (approximately Mason County, Texas). Part (a) illustrates unfiltered height field, $h\,(x,y)$, resolved at $1/9^{th}$ Arc-Seconds. Part (b) illustrates filtered height field after filtering at LES computational mesh resolution, $\tilde{h}\,(x,y)$.

where St_0 and Cd_0 are the interfacial Stanton number and interfacial drag coefficient. The term within the exponential in Equation 6 is often lumped into the parameter, $B^{-1} = St_0^{-1} - Cd_0^{-1/2}$ [22, 23], and named the interfacial transfer coefficient. Numerous models for B^{-1} have been developed, all of which have a dependence on the roughness Reynolds number, $Re_0 = u_\tau z_0/\nu$, as: $St_0^{-1} = \phi_1 Re_0^{\phi_2} Pr^{\phi_3}$. Various groups have offered values for the set of ϕ parameters, while Pr is the Prandtl number. In a recent study, we[24] used an immersed boundary method[25] to model flow over fully-resolved, fractal topographies. Since the topographies were fully-resolved, we could dynamically evaluate the equivalent z_0 during simulation, thereby allowing *a priori* computation of Re_0, St_0, z_{0S} (Equation 6), and then $\dot{q}''$ (Equation 5). The principle finding from this study[24] was that the ratio, z_{0S}/z_0, varied over several orders of magnitude as Re_0 changed; moreover, $z_{0S}/z_0 << 10^{-1}$ for most of the fractal topographies considered. This conflicts somewhat with the commonly-used assumption that $z_{0S}/z_0 = 10^{-1}$, and is consequential for numerical weather prediction of micrometeorological conditions over battlefield environments. This work was largely completed during the interval between original proposal submission and eventual award (Spring, 2012 to Summer, 2013). By the time the grant was awarded, Anderson had developed a strong interest in studying the morphological characteristics of turbulent atmospheric flows over urban environments. At the PM's approval, Anderson effectively allocated Year # 1 of the funding effort to this problem, outlined below.

2 Findings

Turbulent momentum transport in atmospheric boundary layer flows is of critical importance to the performance of modern wind farms[26], aerodynamics of vegetative canopies[27, 9] and urban environments[28, 29, 5, 4], and geomorphological processes associated with evolution of aeolian desert landscapes[30]. These examples are distinctly different to smooth wall turbulence, owing to the presence of a distribution of obstacles of height, h, that protrude into the inertial layer of the flow. These obstacles absorb momentum through pressure drag, induce flow separation and serve to produce obstacle-scale coherent motions that occupy the region between the wall and two to four times the obstacle height – the roughness sublayer[31, 6]. In the roughness sublayer, the vertical aerodynamic drag distribution due to the presence of obstacles results in an inflected

mean streamwise velocity profile at the approximate average obstacle height[8, 32]. As a result, the mean flow gradient exhibits its maxima at the inflection[30] (not the wall), and the turbulence kinematics are fundamentally different. For flow over vegetative canopies, Raupach et al.[33] illustrated that flow in the roughness sublayer resembled a turbulent mixing layer with positively and negatively skewed streamwise and vertical velocity fluctuations, respectively, and Reynolds stresses composed predominately of "sweeps". With this, the turbulence morphology is characterized by Kelvin-Helmholtz spanwise "rollers" which originate at the velocity profile inflection and undergo a downstream metamorphosis leading to hairpin packets [27]. Recently, Ghisalberti[34] demonstrated the existence of an universality in roughness sublayer statistics for flows over diverse canopies, and introduced the term "*obstructed shear flow*" to categorize such flows. Within the sublayer, the turbulence geometric macroscale is effectively set by the vorticity thickness[35, 33], $\delta_w = u_h/(dU/dz)|_h$, and streamwise spacing of vortex cores, $\Lambda_x = 2\pi L_{\ddot{w}}$, where $L_{\ddot{w}}$ is the integral length scale. The mixing efficiency associated with these Kelvin-Helmholtz roughness sublayer motions (sustained by mean flow gradient with maxima at the canopy height) exceeds the analogous value for a logarithmic profile by approximately 50 %. Thus, turbulence in the roughness sublayer is characterized by vigorous mixing and complex structural attributes.

Above the roughness sublayer – in the inertial layer – the mean flow profile exhibits logarithmic scaling and the turbulence structure resembles smooth wall flow[8, 32, 5]. That is, the domain is occupied by persistent streamwise-elongated coherent parcels of relatively low and high momentum regions. For smooth walls, such low momentum regions meander[36], and are encapsulated by hairpin packets[37, 38, 39, 40, 41, 42, 43, 44] at the interface between zones of quasi-uniform momentum[45]. For rough walls, the presence of persistent structures is also reported[5, 42], however experiments have indicated that h-scale coherent motions associated with the roughness sublayer seemingly attenuate the lengths of logarithmic-layer coherent motions[42]. Recently, Coceal *et al.*[5] used direct numerical simulation (DNS) to study flow over a staggered array of uniform height cubes[28] with characteristic scale, $h/H = \frac{1}{4}$, where H is the boundary layer depth. They illustrated the existence of hairpin packets (and "cane" structures: inclined coherent parcel with only one leg of the hairpin[41] around the low momentum region). Moreover, they used approximated conditional averages[46, 37] to illustrate the significant reductions in streamwise coherence of their rough wall turbulence relative to a smooth wall. These efforts to characterize the structural attributes of smooth and rough wall turbulence have typically focused on spatial characteristics. Further, most previous studies address either instantaneous, ensemble-averaged, or time-averaged statistically stationary turbulence statistics. Here, we sought to reconcile spatial and temporal turbulence statistics during flow over urban-like topographies, and topographies with a uniform aerodynamic roughness length. This was accomplished simply by nominating locations throughout the computational domain at which flow statistics are recorded across the depth of the boundary layer in time (thus, we use LES to generate datasets that would more typically be associated with field campaign data from a tower equipped with sonic anemometers)[47].

We used large-eddy simulation (LES) to model flow over topographies composed of a staggered distribution of wall-mounted cubes (one of the cases considered is "C20S" from the wind tunnel study by Cheng and Castro[28], and considered in the more recent DNS study by Coceal et al.[5]). Figure 2(a) shows a perspective view of the array of cubes

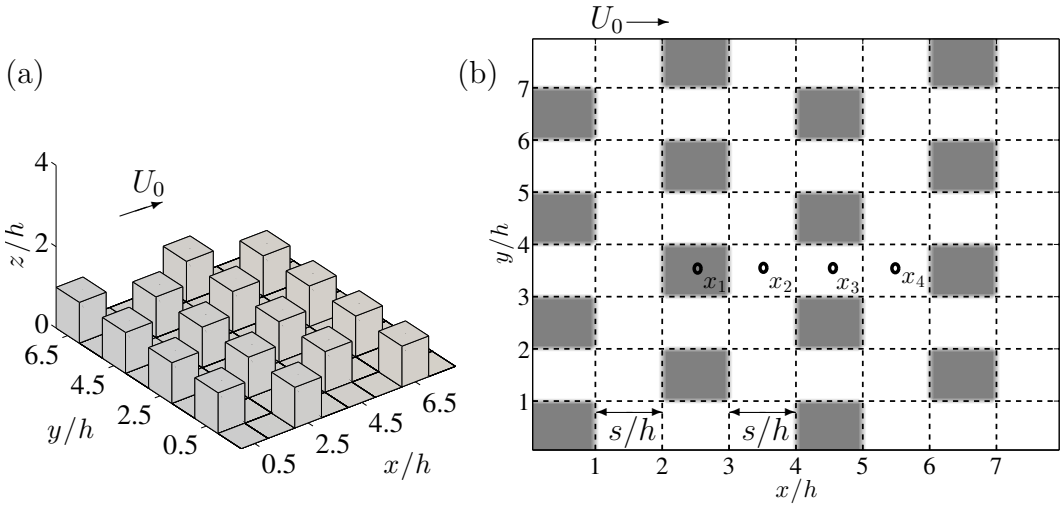

Figure 2: Illustration of [28] block case ("C20S") considered as lower topography in present study: (a) perspective image showing freestream flow direction, U_0; and (b) planform image with indication of positions at which time-height velocity data are recorded. Owing to the topography attributes, the four points effectively capture transient dynamics at all points in the domain. The above topography is labeled here Case SC2.

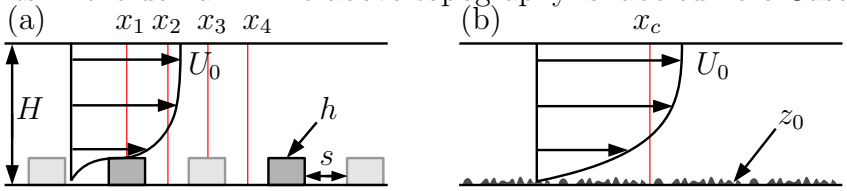

Figure 3: (Color) Illustration of computational domains considered in the present study: (a) uniform height, staggered array of blocks[28] with h varying, $s/h = 1$; and (b) homogeneous roughness, z_0. For Panel (a), see also Figure 2. For all cases, $H = 1000$ m. Illustrative locations of positions at which time-series of streamwise and vertical velocity are recorded are shown for discussion (vertical red lines). In both, an illustrative time-averaged streamwise velocity profile is shown, where U_0 is the "outer" freestream velocity.

with edge length, h. Figure 2(b) shows the arrangement in planform, with indication of the streamwise spacing, s/h, between rows of cubes (here, we consider only cases with $s/h = 1$). Figure 2(b) also includes indication of Points x_1, x_2, x_3, and x_4; during LES, time-series of streamwise and vertical velocity have been recorded across the depth of the boundary layer at these points. This is better illustrated in Figure 3(a), which shows the cubes and streamwise spacing (for the cube cases, the y coordinates of Positions x_1 to x_4 are equal and set to intersect the center of cubes; the x coordinates are varied such that: x_1 is precisely at the center of a cube, x_2 is centered between the upwind and downwind row of cubes, x_3 is precisely at the center of adjacent cubes, and x_4 is centered between the upwind and downwind row of cubes). For generality, we also model flow over homogeneous roughness lengths, shown in Figure 3(b). This work is novel, since it provides datasets that might more readily be retrieved from a micrometeorological tower equipped with sonic anemometers (while retaining the spatial flexibility offered from LES). From adopting such a viewpoint, we can gain deeper insight about the role of coherent structures in the observed time-series phenomena.

Figure 4 shows time-height contour maps of fluctuating velocity component (defined for

this purpose as $\tilde{\boldsymbol{u}}'(\boldsymbol{x},t) = \tilde{\boldsymbol{u}}(\boldsymbol{x},t) - \langle\tilde{\boldsymbol{u}}(\boldsymbol{x},t)\rangle_t$, where $\langle\ldots\rangle_t$ denotes averaging over time, t). For brevity, we show only $\tilde{u}'$ and $\tilde{w}'$ at the limiting positions (i.e. x_1 and x_4), although intermediate values exhibit similar patterns. We also show the same contours for flow over a homogeneous roughness distribution (Figures 4e and 4f). It is clear from inspection that the $\tilde{u}'$ contours exhibit a significant advective lag for all cases; that is, the passage of parcels of relatively high- or low-momentum in the aloft boundary layer precedes "similar" activity in the roughness sublayer. This is further evidenced by consideration of the solid contours, which illustrate Reynolds stresses owing to "sweep" and "ejection" events (determined via quadrant analysis[48]). One can further appreciate that – in general – elevated Reynolds stresses owing to sweeps (vigorous downward excursions of high momentum fluid, into the sublayer) are also preceded by aloft passage of high momentum regions. This is clear evidence that the characteristics of outer layer coherent parcels of fluid are "imprinted" on roughness sublayer processes; moreover, qualitative observations from Figures 4(a), (c), and (e) suggest an advective lag between passage of such outer layer structures and excitation of sublayer dynamics.

We quantify the $\tilde{u}'$ advective lag qualitatively observed in Figure 4. This is accomplished in two steps. Firstly, a reference height, $z_{\text{Ref.}}$, is nominated at which a reference dataset can be collected. We selected $z_{\text{Ref.}}$ to be slightly above the "top" of the roughness. We adopted this approach since it facilitates comparison between these fundamentally different topographies. From here, we compute correlations maps as the convolutions:

$$\gamma(z,\tau) = \left(\tilde{u}'(\boldsymbol{x}_l,z,t) \star \tilde{u}'(\boldsymbol{x}_l,z_{\text{Ref.}},t)\right)(\tau) = \int_{-\infty}^{\infty} \tilde{u}'(\boldsymbol{x}_l,z,t)\tilde{u}'(\boldsymbol{x}_l,z_{\text{Ref.}},t+\tau)dt, \qquad (7)$$

where $\boldsymbol{x}_l$ represents a spatial position (Figure 2b). From this, we compute advective lag as:

$$\tau_{\text{max.}}(z) = \arg\max_t((\tilde{u}'(\boldsymbol{x}_l,z,t) \star \tilde{u}'(\boldsymbol{x}_l,z_{\text{Ref.}},t))(t)), \qquad (8)$$

where we discard $\tau_{\text{max.}}$ values corresponding with $\gamma(z,\tau_{\text{max.}}) < \chi$, where $\chi = 0.3$ is a predefined threshold. We experimented with a range of χ values, finding generally that increasing the threshold only serves to remove spurious values for $z >> z_{\text{Ref.}}$ while the underlying $\tau_{\text{max.}}(z)$ trends were robust and indifferent to χ. Figure 5 shows shear normalized advective lag, $\tau_{\text{max.}}(z)u_\tau H^{-1}$ for Cases SC1, SC2 and U1 (Cases SC1 and SC2 correspond with $h/H = 1/8$ and $= 1/4$, respectively). For Cases SC1 and SC2, it is clear that Positions x_1 to x_4 exhibit effectively the same $\tau_{\text{max.}}u_\tau H^{-1}$ profiles. Above $z_{\text{Ref.}}$, the profiles are roughly linear, and we remind the reader that $z_{\text{Ref.}}$ is the approximate obstacle elevation (or center of the mean streamwise velocity profile inflection). Further, the advective lag is always negative above $z_{\text{Ref.}}$, which is precisely consistent with qualitative observations in Figure 4. For Position x_1, there of course are no $\tau_{\text{max.}}u_\tau H^{-1}$ datapoints below $z_{\text{Ref.}}$ due to the solid cube. A few datapoints are available for Position x_2, owing to its position in the lee of the cubes. However, at Positions x_3 and x_4, there are $\tau_{\text{max.}}u_\tau H^{-1}$ values which illustrate that activity at $z_{\text{Ref.}}$ precedes activity below h and is positively correlated with momentum transport processes in the canopy, not the roughness sublayer. We emphasize also that the $\tau_{\text{max.}}u_\tau H^{-1}$ values in Figure 5 are only associated with γ exceeding threshold, $\chi = 0.3$. Thus, the approximate linearity, $\tau_{\text{max.}} \sim -z$ for $z > z_{\text{Ref.}}$, is a product of actual processes within the roughness sublayer and inertial layer.

The presence of meandering, coherent parcels of relatively low and high momentum in turbulent wall-bounded flows over smooth[37, 38, 39, 40, 41, 43, 44] and rough[5, 42] walls

is well known. The low momentum regions (LMR) are encapsulated by hairpin packets at the interface between regions of differing momentum[45, 41]. For the case of cube roughness such as the cases considered here, Figure 6 is a sketch of the aforementioned structural attributes. A streamwise-vertical transect through a LMR would reveal a typical inclination of $\gamma \approx 15°$[37, 42]. Quantitative visualization of the Figure 6 dynamics can also be attained with vortex visualization techniques (excluded here, for brevity). Figure 5 shows vertical profiles of advective lag, $\tau_{\max.} u_\tau H^{-1}$, based on a reference elevation just above the canopy (see Figure 5). The linearity exhibited by $\tau_{\max.} u_\tau H^{-1}$ points to an underlying physical process in the roughness sublayer and inertial layer. We attribute $\tau_{\max.} \sim -z$ scaling to the passage of regions of alternating low and high momentum in the roughness sublayer and inertial layer.

Following the passage of a LMR, the first position in the domain to experience relatively higher momentum would be in the inertial layer, above the LMR. As the LMR advects downstream, relatively higher momentum would be recorded at progressively lower elevations. In keeping with the viewpoint adopted thus far, time-series measurement of flow statistics throughout the domain at a position upwind of the LMR, x_1, would experience low momentum higher in the domain first. The LMR would be observed at progressively lower z with increasing time. The above pattern would be true for regions of relatively high momentum too. Since *representative* information is known about the macroscale attributes of these coherent motions, we have developed a simple, semi-empirical model to predict the advective lag between passage of such motions in the inertial layer and evidence of their "imprint" on roughness sublayer and canopy dynamics.

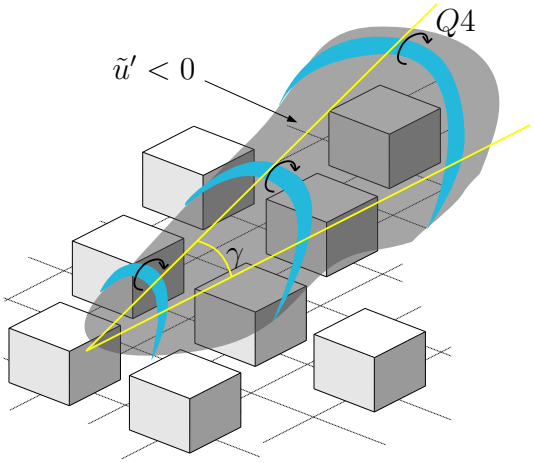

Figure 6: (Color) Sketch of low momentum region (LMR) above array of cubes. The LMR, $\tilde{u}' < 0$, is denoted by transparent gray. Encapsulating the LMR are hairpins (blue). The LMR is inclined at angle, γ, and the hairpin heads exhibit positive transverse vorticity (sketch denotes sweep event, $Q4$). The individual hairpin "legs" would themselves be inclined at $\approx 45°$[41].

If a LMR (i.e. $\tilde{u}' < 0$, above) has depth, δ', its length can be evaluated based on assumption of a hairpin train inclination angle:

$$L_s \approx \delta' / \tan(\gamma) \,. \tag{9}$$

Furthermore, if we assume that a representative advective velocity for low and high momentum regions is the "outer" velocity, U_0, we can use the equilibrium logarithmic law[49] and aerodynamic roughness length, z_0, to predict U_0:

$$\frac{U_0}{u_\tau} = \frac{1}{\kappa} \log\left[\frac{H}{z_0}\right] . \tag{10}$$

$\tau_{\max.}(z)$ is the advective lag between passage of a coherent motion at elevation, z, and associated modulation of processes at reference height, $z_{\text{Ref.}}$. Thus, Equations 9 and 10

can be combined to obtain the advective lag:

$$\tau_{\max.}(z) = \frac{z - z_{\text{Ref.}}}{\tan(\gamma)\, U_0} = \frac{\kappa(z - z_{\text{Ref.}})}{\tan(\gamma)\, u_\tau \log(H/z_0)}. \tag{11}$$

Normalizing $\tau_{\max.}(z)$ by friction velocity and boundary depth ("shear normalized") yields:

$$\tau_{\max.}(z) u_\tau H^{-1} = \frac{\kappa\,(z - z_{\text{Ref.}})}{\tan(\gamma)\, H \log(H/z_0)}. \tag{12}$$

We have used the LES data to evaluate $z_{0,\text{Eff.}}$ for the block cases ($h/H = 1/8$ and $= 1/4$), enabling prediction of the outer velocity, U_0, if assuming that the inertial layer profile retains a logarithmic form to $z = z_0$. Alternatively, one could use predictive models for z_0 based on attributes of the topography[50, 51, 1] although this would require empirical parameters[52]. For Cases SC1, SC2, and U1, Figure 5 shows predictions from Equation 12 (solid lines). For $z_{\text{Ref.}}/H \lesssim z/H \lesssim 0.2$, Equation 12 predictions exhibit reasonable agreement with the LES results for Case U1. This is the case of homogeneous roughness in which the roughness sublayer may be $z/H \lesssim 0.1$. For Cases SC1 and SC2, Equation 12 predictions agree somewhat well with the LES data for $z_{\text{Ref.}}/H \lesssim z/H \lesssim 0.4$, corresponding with 2 to 4 times the cube height. Thus, the model performance is moderately successful in the roughness sublayer and into the inertial layer.

3 Dissemination

The work described above (from Year # 1 of the research effort) has been presented through invited seminars, conference talks/proceedings, and peer review publications. Although the material described in Section 1 (passive scalar fluxes from fractal topography) was performed before the funding period began, we include dissemination of this material below as part of the "outcomes" since it was discussed in the original proposal.

Invited Talks:

- August, 2014: Microscale Atmospheric Dynamics Branch, Army Research Laboratory, Adelphi, MD.
- June, 2014: Summer Institute on Medicine and Energy, Texas Tech University.
- March, 2014: Mechanical Science and Engineering Department, University of Illinois at Urbana-Champaign.
- March, 2014: Mechanical Engineering Department, University of Texas at Austin.
- March, 2014: Sandia National Laboratory, Albuquerque, NM.
- February, 2014: Mechanical Engineering Department, University of Texas at San Antonio [Declined].
- January, 2014: Mechanical Engineering Department, University of Texas at Dallas.
- January, 2014: Extreme Fluids Group, Los Alamos National Laboratory, Los Alamos, NM.

- July, 2013: Army Research Laboratory, Atmospheric Dynamics Branch.
- March, 2013: Texas Tech University, Department Mechanical Engineering, Lubbock, TX.
- February, 2013: Aerospace Engineering and Engineering Mechanics, the University of Texas at Austin, Austin, TX.
- 2012: September, 2012: Baylor University, Mechanical Engineering Department.

Conference Proceedings:

- Anderson W, Li Q, Bou-Zeid E, 2014: *Proc. of American Geophysical Union, Fall Meeting, San Francisco, CA*.
- Anderson W, Li Q, Bou-Zeid E, 2014: *Proc. of American Physical Society, Division of Fluid Dynamics, San Francisco, CA*.
- Li Q, Bou-Zeid E, Anderson W, 2014: *Proc. of American Physical Society, Division of Fluid Dynamics, San Francisco, CA*.
- Anderson W, Li Q, Bou-Zeid E, 2014: *Proc. of American Meteorological Society, Symposium on Boundary Layers and Turbulence, Leeds, England.*
- Li Q, Bou-Zeid E, Anderson W, 2014: *Proc. of American Meteorological Society, Atlanta, GA*.
- Anderson W, 2012: *Proc. of American Meteorological Society, Symposium on Boundary Layers and Turbulence, Boston, MA*.
- Anderson W, Passalacqua P, 2012: *Proc. of American Meteorological Society, Symposium on Boundary Layers and Turbulence, Boston, MA*

Peer-Review Journal:

- Anderson W, 2013: Passive scalar roughness lengths for atmospheric boundary layer flow over complex, fractal topographies. *Environmental Fluid Mechanics* **13**, 479-501.
  Summary: This manuscript outlines the material is Section 1, showing that z_{0S}/z_0 can be $<< 10^{-1}$ for multiscale, fractal topographies.
- Anderson W, Li Q, Bou-Zeid E, 2014: Transient dynamics of coherent motions in an urban-like roughness sublayer. *Journal of Turbulence (Under Review).*
  Summary: This manuscript presents the material briefly described in Section 2. The manuscript was submitted on July 10, 2014.

4 Fiscal

The Year # 1 budget was $40,000, which supported the following items:

- Travel by Anderson to the American Meteorological Society, Symposium on Boundary Layers and Turbulence in Leeds, UK
- Two months of summer salary for Anderson

- Modest equipment and publishing budget

In Years # 2 (FY15) and # 3 (FY16), the award will provide $76084 and $34840, respectively. These funds will support Anderson summer salary, travel, and research stipend for a new doctoral candidate (Xiaowei Zhu, previously a research associate at Nanyang Technological University, Singapore). Comprehensive details of expenses and fund allocations have been provided on the full proposal submitted to ARO in 2014, as part of Anderson's new start at UTD.

5 Upcoming

Year # 2 of the project (Year # 1 of the UT Dallas new start award) will focus on evaluating the transient dynamics of flows over more complex topographies (i.e. beyond staggered, uniform height cubes) in the context of the existing Section 2 insights. That is: how does spacing or variable height, for example, affect the Equation 9 to 12 development. In fact, the topic of spacing is already "underway" through a collaboration between Anderson and Elie Bou-Zeid, Princeton University. Elie and his student, Qi Li, have studied the transient dynamics questions with spacing varied above and below the cases considered here. In addition, we will begin to consider the effects of fractal topographies (with varying spectral exponent, or fractal dimension), to evaluate how varying "roughness" modifies the spatial extent of coherent parcels of fluid. Townsend's outer layer similarity hypothesis states that smooth and rough wall turbulence statistics should be invariant in the outer layer[53]. Some recent efforts have demonstrated that complex roughness serves to attenuate coherence in the roughness sublayer[5, 42], while Hong et al.[54] demonstrated a persistent "near wall" signature in outer layer turbulence statistics for flow over a distribution of pyramids. Thus, by considering a suite of fractal topographies with varying fractal dimension, we could determine the presence of monotonic trends in turbulence morphology with additional geometric complexity of the underlying topography.

6 Institutional Move: Baylor University to the University of Texas at Dallas

Anderson completed his PhD (Mechanical Engineering) at The Johns Hopkins University in July, 2011, and began as a tenure-track faculty in the Mechanical Engineering Department at Baylor University in Fall, 2011. Anderson greatly enjoyed being at Baylor, but experienced acute difficulty recruiting graduate students. This was exacerbated by virtue of federal grants awarded and a growing research portfolio (please see Section 7); in fact, Anderson in one case had to decline significant funds because they could never have been expended. Thus, Anderson was in the unfortunate situation of having to move to an institution with a more matured research enterprise. In July, 2014, Anderson moved to the Mechanical Engineering Department at The University of Texas at Dallas.

7 Additional Funding

In the interest of openness, Anderson has below provided a list of active and pending grants, and a brief summary of the research. Anderson will also gladly provide contact information for the respective program manager at ARO's request[†].

[†]Note that this list excludes white papers presently under review or external consulting activities.

- $240000: Air Force Office of Scientific Research, Young Investigator Program (October, 2014 - September, 2017)
  Summary: This AFOSR award will support a new topic studying the role of canonical roughness in sustaining mean secondary flows within a turbulent boundary layer.

- $20000: Shell Exploration and Production Company (January, 2014 - December, 2014)
  Summary: This industrial grant supports efforts to model atmospheric surface layer flows over fields of aeolian sand dunes. The work is motivated by the need to understand aerodynamic stresses responsible for geomorphic evolution of dune fields.

- $1.2 million: Air Force Office of Scientific Research, Turbulence and Transition Program (July, 2014 - June, 2018)
  Summary: This award is to be divided between Anderson and collaborators (K. Christensen, Notre Dame, and C. Pantano, UIUC). The award focuses on refinement of wall models for large-eddy simulation of rough wall turbulent boundary layers. The refinement here will be accomplished by adaptation of 'Amplitude Modulation' concepts – developed recently for smooth wall flows by Ivan Marusic and collaborators – for flows over rough surfaces.

- Under Review: National Science Foundation, CAREER (Fluid Dynamics Program, CBET) (September, 2015-August, 2020)
  Summary: This project will support a more detailed study of turbulence processes in dune field environments (that is, development of bulk characterizations of the turbulent mixing-layer like processes present in close proximity to the dunes). This work will especially focus on "realistic" aeolian dune fields, with spatial distribution set by winds from multiple directions.

- Under Review: National Science Foundation, Physical and Dynamic Meteorology Program (GEO)
  Summary: Anderson has submitted a DoD-style white paper to this program for consideration. At the program manager's request, Anderson is now developing a full proposal. The project will focus on the morphology of coherent turbulent parcels in the convectively stratified atmospheric boundary layer, and their role in intermittent surface fluxes of dust from arid landscapes on the Llano Estacado in west Texas and eastern New Mexico.

- Under Review: National Science Foundation, Fluid Dynamics Program (CBET)
  Summary: Anderson (as co-PI) and collaborators (PI K. Christensen, University of Notre Dame; co-PI Gianluca Blois, University of Notre Dame; co-PI J. Best, University of Illinois at Urbana-Champaign; co-PI G. Kocurek, University of Texas at Austin), have submitted a full proposal to the NSF-ENF-CBET-Fluid Dynamics Program that focuses on turbulent flows over canonical barchan dunes. The proposal is an experimental-numerical collaborative. The three-year budget request was $540,000, of which Anderson will receive $180,000.

- Under Review: Texas Department of Transportation (TXDoT), Research and Technology Implementation Office (RTI)

Summary: A three-year project is under review at TXDoT with Anderson as the sole PI. The project will use the Weather Research and Forecasting (WRF) computation package for modeling mesoscale meteorological conditions and using short term forecasts to inform trafficability in Texas.

- To be Submitted: Office of Naval Research, Young Investigator Program (Programmatic Area: Hull Performance/Undersea Hydromechanics)
  Summary: This research is complimentary to aspects of this ongoing ARO project. In this effort, the LES channel flow code will be used to model flow over a suite of complex, fractal (and multifractal) topographies to evaluate how modifying geometric attributes of the synthetic topographies affects the turbulence statistics.

8 Army Research Laboratory Collaborations

Anderson visited the Army Research Laboratory Headquarters in Adelphi, MD in July, 2013 and August, 2014. The 2014 visit was also intended as a "status update" to staff scientists there who were keenly aware of Anderson's research (Drs. Yansen Wang, Ben MacCall, Cheryl Klipp, Chatt Williamson, and Sandra Collier). In addition to discussing Anderson's activities, there is always in-depth discussion about non-secure research being conducted there. Anderson and Ben MacCall continue to explore potential collaboration opportunities in diverse turbulence problems.

References Cited

[1] W. Anderson and C. Meneveau. A dynamic large-eddy simulation model for boundary layer flow over multiscale, fractal-like surfaces. *J. Fluid Mech.*, 679:288–314, 2011.

[2] W. Anderson, P. Passalacqua, F. Porté-Agel, and C. Meneveau. Large-eddy simulation of atmospheric boundary layer flow over fluvial-like landscapes using a dynamic roughness model. *Boundary-Layer Meteorol.*, 144:263–286, 2012.

[3] I. Rodríguez-Iturbe and A. Rinaldo. *Fractal river basins: chance and self-organization.* Cambridge University Press, Cambridge, USA, 1997.

[4] Z.-T. Xie, O. Coceal, and I.P. Castro. Large-eddy simulation of flows over random urban-like obstacles. *Boundary-Layer Meteorol.*, 129:1–23, 2008.

[5] O. Coceal, A. Dobre, T. G. Thomas, and S.E. Belcher. Structure of turbulent flow over regular arrays of cubical roughness. *J. Fluid Mech.*, 589:375–409, 2007.

[6] Margi Böhm, John J. Finnigan, Michael R. Raupach, and Dale Hughs. Turbulence structure within and above a canopy of bluff elements. *Boundary Layer Meteorol.*, 146:393–419, 2013.

[7] M. Bohm, J.J. Finnigan, and M.R. Raupach. Dispersive fluxes and caopy flows: Just how important are they? *Proc. 24th Conf. on Agr. and Forest Meteorol., American Meteorol. Soc., Davis, Calif.*, pages 106–107, 2000.

[8] M.R. Raupach, R.A. Antonia, and S. Rajagopalan. Rough-wall turbulent boundary layers. *Appl. Mech. Rev.*, 44:1–25, 1991.

[9] S.E. Belcher, I.N. Harman, and J.J. Finnigan. The wind in the willows: flows in forest canopies in complex terrain. *Ann. Rev. Fluid Mech.*, 44:479–504, 2012.

[10] J. Finnigan. Turbulence in plant canopies. *Ann. Rev. Fluid Mech.*, 32:519–571, 2000.

[11] M. Germano, U. Piomelli, P. Moin, and W. Cabot. A dynamic subgrid-scale eddy viscosity model. *Phys. Fluids A*, 3:1760–1765, 1991.
[12] A.S. Monin and A.M. Obukhov. Basic laws of turbulent mixing in the ground layer of the atmosphere. *Tr. Geofiz. Inst., Akad Nauk SSSR*, 151:163–187, 1954.
[13] Vijayant Kumar, Jan Kleissl, Charles Meneveau, and Marc B. Parlange. Large-eddy simulation of a diurnal cycle of the atmospheric boundary layer: Atmospheric stability and scaling issues. *Water Resour. Res.*, 42:W06D09, 2006.
[14] H.U. Sverdrup. On the evaporation from the oceans. *J. Marine Res.*, 1:3–14, 1937.
[15] W. Brutsaert. A model for evaporation as a molecular diffusion process into a turbulent atmosphere. *J. Geophys. Res.*, 70:5017–5024, 1965.
[16] W. Brutsaert. A theory for local evaporation (or heat transfer) from rough and smooth surfaces at ground level. *Water Resour. Res.*, 11:543–550, 1975.
[17] P.R. Owen and W.R. Thomson. Heat transfer across rough surfaces. *J. Fluid Mech.*, 15:321–334, 1963.
[18] N. Sheriff and P. Gumley. Heat-transfer and friction properties of surfaces with discrete roughness. *Int. J. Heat and Mass Transfer*, 9:1297–1320, 1966.
[19] D.F. Dipprey and R.M. Sabersky. Heat and momentum transfer in smooth and rough tubes at various prandtl numbers. *Int. J. Heat Mass Transfer*, 6:329–332, 1963.
[20] A.C.M. Beljaars and A.A.M. Holtslag. Flux parameterization over land surfaces for atmospheric models. *J. Appl. Meteor.*, 30:327–341, 1991.
[21] A.T. Cahill, M.B. Parlange, and J.D. Albertson. On the brutsaert temperature roughness length model for sensible heat flux estimation. *Water Resour. Res.*, 33:2315–2324, 1997.
[22] A.M. Yaglom and B.A. Kader. Heat and mass transfer between a rough wall and turbulent fluid flow at high reynolds and peclet numbers. *J. Fluid Mech.*, 62:601–623, 1974.
[23] W. Brutsaert. *Evaporation into the atmosphere*. Kluwer Academic Publishers, Norwell, MA, 1982.
[24] W. Anderson. Passive scalar roughness lengths for atmospheric boundary layer flow over complex, fractal topographies. *Env. Fluid Mech.*, pages DIO 10.1007/s10652–013–9272–9, 2013.
[25] W. Anderson. An immersed boundary method wall model for high-reynolds number channel flow over complex topography. *Int. J. Numer. Methods Fluids*, 71:1588–1608, 2012.
[26] M. Calaf, M.B. Parlange, and C. Meneveau. Large eddy simulation study of scalar transport in fully developed wind-turbine array boundary layers. *Phys. Fluids*, 23:126603–16, 2011.
[27] J.J. Finnigan, R.H. Shaw, and E.G. Patton. Turbulence structure above a vegetation canopy. *J. Fluid Mech.*, 637:387–424, 2009.
[28] H. Cheng and I.P. Castro. Near wall flow over urban-like roughness. *Boundary-Layer Meteorol.*, 104:229–259, 2002.
[29] S.E. Belcher, N. Jerram, and J.C.R. Hunt. Adjustment of a turbulent boundary layer to a canopy of roughness elements. *J. of Fluid Mech.*, 488:369–398, 2003.
[30] W. Anderson and M. Chamecki. *Physical Review E*, 89:013005–1–14, 2014.
[31] Ian Harmon and John J. Finnigan. A simple unified theory for flow in the canopy and roughness sublayer. *Boundary Layer Meteorol.*, 123:339–364, 2007.
[32] I.P. Castro. Rough-wall boundary layers: mean flow universality. *J. Fluid Mech.*, 585:469–485, 2007.

[33] M.R. Raupach, J.J. Finnigan, and Y. Brunet. Coherent eddies and turbulence in vegetation canopies: the mixing layer analogy. *Boundary-Layer Meteorol.*, 78:351–382, 1996.
[34] M. Ghisalberti. Obstructed shear flows: similarities across systems and scales. *J. Fluid Mech.*, 641:51, 2009.
[35] M.M. Rogers and R.D. Moser. Direct simulation of a self-similar turbulent mixing layer. *Phys. Fluids A*, 6:903–922, 1994.
[36] N. Hutchins and I. Marusic. *J. Fluid Mech.*, 579:1–28, 2007.
[37] J. Zhou, R.J. Adrian, S. Balachandar, and T.M. Kendall. Mechanisms for generating coherent packets of hairpin vortices in channel flow. *J. Fluid Mech.*, 387:353–359, 1999.
[38] R.J. Adrian, C.D. Meinhart, and C.D. Tomkins. Vortex organization in the outer region of the turbulent boundary layer. *J. Fluid Mech.*, 422:1–54, 2000.
[39] K.T. Christensen and R.J. Adrian. Statistical evidence of hairpin vortex packets in wall turbulence. *J. Fluid Mech.*, 431:433–443, 2001.
[40] B. Ganapathisubramani, E. K. Longmire, and I. Marusic. *J. Fluid Mech.*, 478:35–46, 2003.
[41] R.J. Adrian. *Phys. Fluids*, 19:041301, 2007.
[42] Y. Wu and K. T. Christensen. Spatial structure of a turbulent boundary layer with irregular surface roughness. *J. Fluid Mech.*, 655:380–418, 2010.
[43] D.J.C. Dennis and T.B. Nickels. *J. Fluid Mech.*, 673:180–217, 2011.
[44] D.J.C. Dennis and T.B. Nickels. *J. Fluid Mech.*, 673:218–244, 2011.
[45] C.D. Meinhart and R.J. Adrian. On the existence of uniform momentum zones in a turbulent boundary layer. *Phys. Fluids*, 7:694–696, 1995.
[46] R.J. Adrian. Linking correlations and structure: stochastic estimation and conditional averaging. In *Zoran P. Zaric Memorial International Seminar on Near-Wall Turbulence*. Hemisphere, 1988.
[47] W. Anderson, J. Barros, and K. T. Christensen. *J. Fluid Mech.*, page Under Rev., 2014.
[48] S.S. Lu and W.W. Willmarth. Measurements of the structure of reynolds stress in a turbulent boundary layer. *J. Fluid Mech.*, 60:481–571, 1973.
[49] U. Piomelli and E. Balaras. Wall-layer models for large-eddy simulation. *Ann. Rev. Fluid Mech.*, 34:349–374, 2002.
[50] J.R. Garratt. *The atmospheric boundary layer*. Cambridge University Press, UK, 1994.
[51] M.V. Zagarola and A.J. Smits. Mean-flow scaling of turbulent pipe flow. *J. Fluid Mech.*, 373:33–79, 1998.
[52] M.P. Schultz and K.A. Flack. Turbulent boundary layers on a systematically-varied rough wall. *Phys. Fluids*, 21:015104, 2009.
[53] A.A. Townsend. *The structure of turbulent shear flow*. Cambridge University Press, Cambridge, UK, 1976.
[54] J. Hong, J. Katz, C. Meneveau, and M. Schultz. Coherent structures and associated subgrid-scale energy transfer in a rough-wall channel flow. *J. Fluid Mech.*, 712:92–128, 2012.

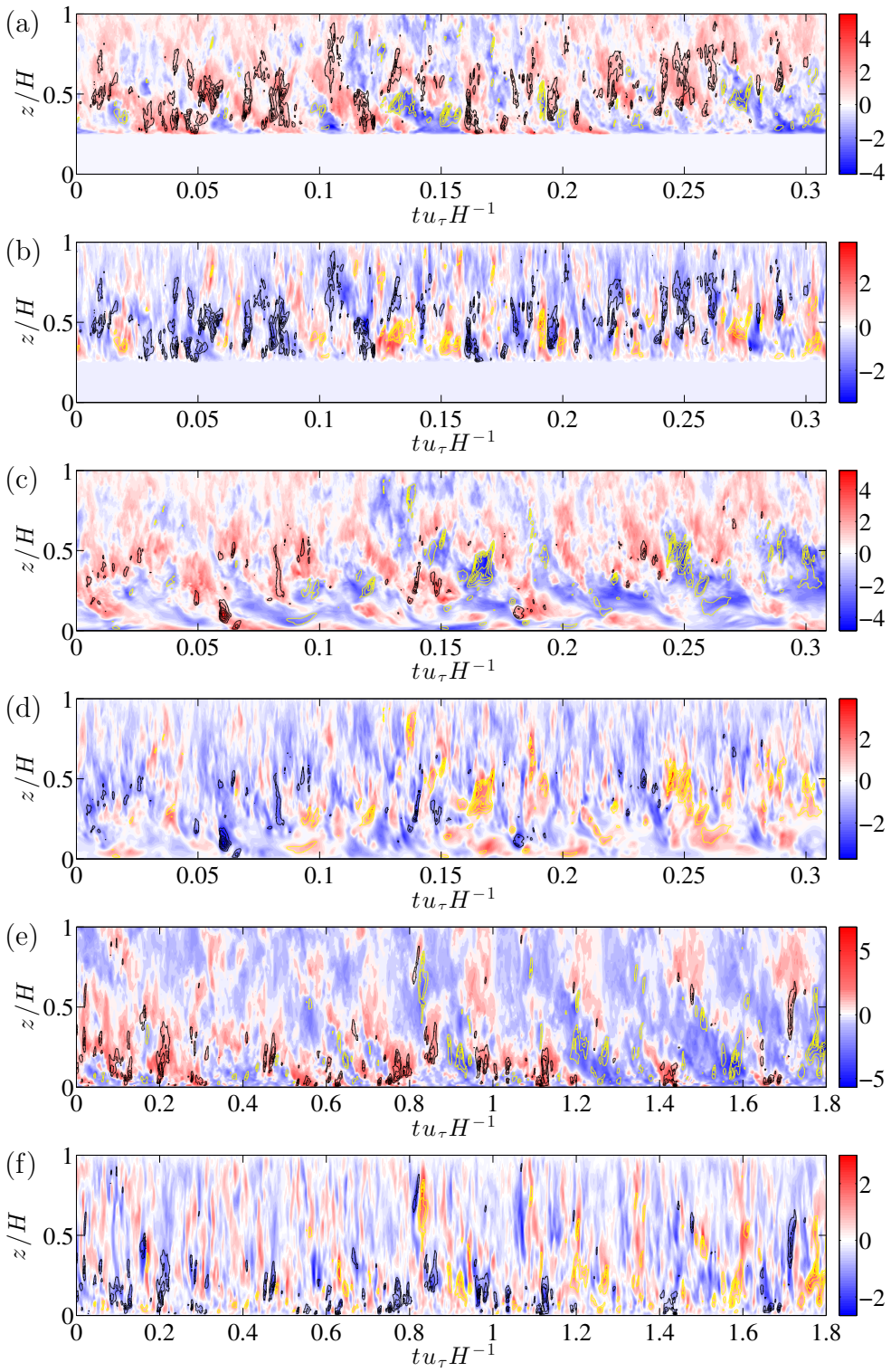

Figure 4: (Color) Time-height contours of fluctuating velocity ($\tilde{\boldsymbol{u}}'(\boldsymbol{x},t) = \tilde{\boldsymbol{u}}(\boldsymbol{x},t) - \langle\tilde{\boldsymbol{u}}(\boldsymbol{x},t)\rangle_t$) components for flow over cubical topography (Panels a-d) and homogeneous roughness (Panels e and f) at positions indicated in Figure 3: (a) $\tilde{u}'(x_1,y_1,z,t)$ at x_1; (b) $\tilde{w}'(x_1,y_1,z,t)$ at x_1; (c) $\tilde{u}'(x_4,y_4,z,t)$ at x_4; (d) $\tilde{w}'(x_4,y_4,z,t)$ at x_4; (e) $\tilde{u}'(x_c,y_c,z,t)$ at center; and (f) $\tilde{w}'(x_c,y_c,z,t)$ at center. In addition to color floods, line contours denote contribution to $\tilde{u}'\tilde{w}'$ due to $Q4$ "sweep" (black) and $Q2$ "ejection" (yellow) events. Note that in Parts (a) and (b), $\tilde{\boldsymbol{u}}'(x,y,z/H<1/4,t)=0$ owing to the presence of cubes of height $h/H=1/4$

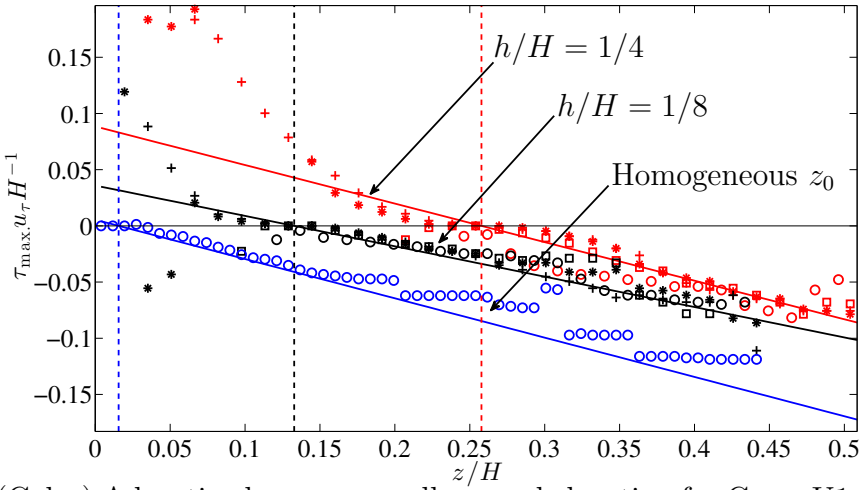

Figure 5: (Color) Advective lag versus wall-normal elevation for Cases U1 (blue symbols), SC1 (black symbols), and SC2 (red symbols). For Cases SC1 and SC2, symbols correspond with: x_1 (circles), x_2 (squares), x_3 ("plus" sign), and x_4 (asterisk). Blue symbols correspond with x_c for the homogeneous rough case. Vertical dashed lines denote $z_{\text{Ref.}}$ for different cases (dashed blue: U1; dashed black: SC1; and dashed red: SC2). Solid lines represent Equation 12 predictions of time-lag for effective roughness lengths determined *a posteriori* from simulations.